Magnetic characterization of the Peierls transition of di-naphthalene hexafluoroarsenate

2002 J. Phys.: Condens. Matter 14 8655

(http://iopscience.iop.org/0953-8984/14/37/302)

INSTITUTE OF PHYSICS PUBLISHING JOURNAL OF PHYSICS: CONDENSED MATTER

J. Phys.: Condens. Matter **14** (2002) 8655–8662 PII: S0953-8984(02)38057-3

Magnetic characterization of the Peierls transition of di-naphthalene hexafluoroarsenate

Barbara Pongs, Gerda Fischer and Elmar Dormann

Physikalisches Institut, Universität Karlsruhe (TH), 76128 Karlsruhe, Germany

Received 12 June 2002, in final form 31 July 2002
Published 5 September 2002
Online at stacks.iop.org/JPhysCM/14/8655

Abstract

The magnetic susceptibility of the prototype of quasi-one-dimensionally conducting arene radical cation salts, the naphthalene salt $(C_{10}H_8)_2AsF_6$, is analysed. The Peierls transition is characterized by a molecular field temperature T_{MF} of about 570 K and an actual three-dimensional transition temperature T_P of 234 ± 4 K. The low-temperature gap is extrapolated to $2\Delta(0)/k_B = 1950 \pm 75$ K. The naphthalene salt thus has the highest Peierls transition temperature among the arene radical cation salts analysed so far.

1. Introduction

Currently, the general interest in Luttinger liquids is strongly reviving, and several authors are tending to the view that quasi-one-dimensional conductors such as the Bechgaard salts exhibiting a low-temperature spin–Peierls transition temperature might present an experimental realization of various models considered [1–3]. In this connection, with this contribution we want to recall to attention the fact that many extremely anisotropic quasi-one-dimensional conductors that exhibit $\sigma_\parallel/\sigma_\perp$ up to 10^4:1 and in addition show highly one-dimensional π-molecular overlap patterns of stacked flat aromatic pure hydrocarbon molecules (arenes) actually show charge-density-wave (CDW) fluctuations and a CDW–Peierls transition [4, 5], as suggested long ago [6, 7]. It has not been possible to unravel any difference between charge and spin motion in such systems up to now, at least on the microsecond timescale [8, 9]. This indicates that electron–phonon interaction predominates in the arene radical cation salts rather than electron–electron interaction, presumably due to the low local π-electron density at the various carbon sites of arene radical cations. In fact, it was also concluded that the transition to the long-range three-dimensionally ordered state in PF_6 and AsF_6 systems is triggered by three-dimensional phonon coupling via the anions [10].

Under these circumstances, it is highly regrettable that the Peierls transition of the prototype of the arene radical cation salts, the $(naphthalene)_2X$ salt with X = PF_6 or AsF_6 anions, has not yet been characterized in any detail [11, 12]. This may be due to the poor stability of these crystals, related in part to the high vapour pressure of naphthalene. This will be remedied with the current analysis. In fact, naphthalene $C_{10}H_8$, abbreviated as NA in the

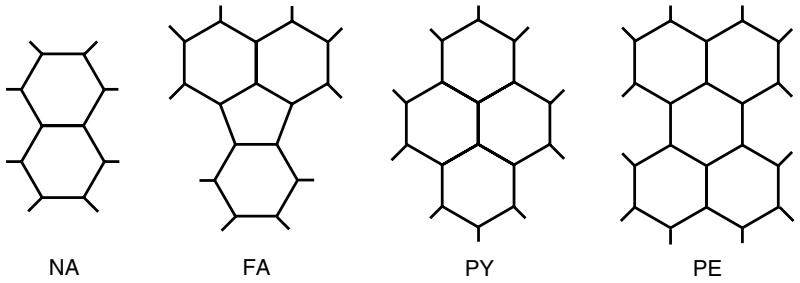

Figure 1. A sketch of the arenes considered in this paper: naphthalene, $C_{10}H_8$ (NA), fluoranthene, $C_{16}H_{10}$ (FA), pyrene, $C_{16}H_{10}$ (PY), and perylene, $C_{20}H_{12}$ (PE).

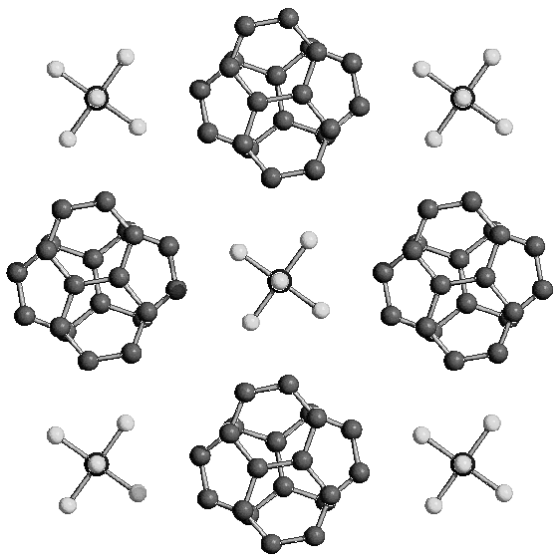

Figure 2. The projection of the crystal structure of $(NA)_2PF_6$ on the *a*–*b* plane [11]

following, is the smallest of the arenes useful for tailoring quasi-one-dimensional conductors (figure 1). Hole concentrations up to 2.3×10^{21} cm^{-3} are achieved in the arene conduction band of the stoichiometric salt. The intrastack NA separation is only 3.20 Å in the PF_6 salt and 3.19 Å in the AsF_6 salt [11]. The $\Delta\varphi = 90°$ rotation of subsequent NA molecules in the one-dimensional stacks (referred to as the 'stacking angle' in table 2, later on) yields optimum volume filling and favourable π-orbital overlap (figure 2) along the *c*-direction of the tetragonal unit cell (space group $P4_2/n$ [11]). Because two NA molecules thus form the periodicity unit in the *c*-direction, the conduction band Brillouin zone is divided in half. Thus, in the high-temperature phase of $(NA)_2AsF_6$, instead of the three-quarter-filled conduction band of the extended band scheme, a half-filled upper band is subject to the influence of the Peierls CDW-like fluctuations. The subsequent strong temperature dependence of the conduction electron magnetic susceptibility is determined below and analysed quantitatively. The highest Peierls transition temperature T_P of about 234 K is derived for $(NA)_2AsF_6$ and compared to those for other arene salts. This agrees with expectation based on crystal structure analysis [11]: it indicates, via the twisting of naphthalene and counterion molecules (figure 2), the action

Table 1. Data derived for two independent samples of nominally $(NA)_2AsF_6$ ($M_m = 445.3$ g) by analysis of the magnetic data.

Sample (weight)	Age (weeks)	$x_{S=1/2}$/f.u.	χ_{dia} (10^{-7} emu g^{-1})	χ_P (10^{-6} emu/445.3 g)	T_{MF} (K)	T_P (K)	Δk_B^{-1} (K)
A (83.3 mg)	5	9.1×10^{-4}	−5.87	102.5	632	238	1015
B (80.8 mg)	10	1.0×10^{-3}	−5.31	62.3	515	238	940

Table 2. The Peierls transition of radical cation salts of the arenes naphthalene (NA), fluoranthene (FA), pyrene (PY), and perylene (PE), exhibiting different molecular or ionic stoichiometries, conduction band fillings (in the extended band scheme), and arene stacking angles. T_{MF}^{χ} is derived from the temperature dependence of the conduction electron magnetic susceptibility, T_P from the Peierls transition anomaly (e.g. of microwave conductivity).

Stoichiometry		Band filling		Stacking angle			
Molecular	Ionic	$k_F^{ext}/\pi\bar{d}^{-1}$	Composition	$\Delta\varphi$ (deg)	T_{MF}^{χ} (K)	T_P (K)	References
2:1	2:1	3/4	$(NA)_2^{\bullet+}AsF_6^-$	90	574 ± 58	234 ± 4	This work
2:1	2:1	3/4	$(FA)_2^{\bullet+}PF_6^-$	180	425	186 ± 6	[14, 15, 17]
11:4	7:4	5/7	$(PY)_7^{4(\bullet+)}(PY^\circ)_4(AsF_6^-)_4$ ·4(CH_2Cl_2) mod. I	0/60	220	73 ± 4	[20, 21]
12:7	12:7	17/24	$(PY)_{12}^{7(\bullet+)}(SbF_6^-)_7$	0	290	116 ± 2	[20, 21]
2:1	4:3	5/8	$(PE)_4^{3(\bullet+)}(PE^\circ)_2(PF_6^-)_3$ ·2(C_4H_80)	0	273	118 ± 2	[10, 18]
2:1	4:3	5/8	$(PE)_4^{3(\bullet+)}(PE^\circ)_2(AsF_6^-)_3$ ·2(C_4H_80)	0	253	102 ± 2	[10, 18]
4:3	4:3	5/8	$(PE)_4^{3(\bullet+)}(SbF_6^-)_3$	0	330	<30	[18, 19]

of substantial NA–AsF_6–NA interactions occurring even at room temperature. This is known to favour the three-dimensional coupling of the 1D-CDW fluctuations and thus to trigger the transition to the 3D-ordered low-temperature phase [10].

2. Experimental details

The $(NA)_2AsF_6$ crystals were grown by anodic oxidation of a solution of naphthalene and tetra-*n*-butylammonium–AsF_6 salt in CH_2Cl_2 at $T = -40\,^\circ$C according to the established rules of electrocrystallization of arene radical cation salts [11, 13]. After growth, before measurement, the samples were stored in a freezer ($T = -17\,^\circ$C). Nevertheless, they slowly decompose, as is noticeable from the evolving dull and colourless surface layers on the originally dark-violet crystals. However, 'stable crystals' could be used in electron-spin-resonance measurements even several weeks after growth. In order to characterize the influence of sample ageing on the static magnetic properties measured and analysed in this contribution, two samples, A and B, consisting of many non-oriented crystals originating from different crystal growth runs, were used, clearly differing in average age (table 1). In addition, in one run the measuring temperature was raised to 320 K in order to monitor the influence of sample decomposition on the magnetic data analysed. Sample history does not influence any relevant parameter by more than 20%; thus the outstanding value of the Peierls transition temperature of $(NA)_2AsF_6$ is beyond question (tables 1 and 2).

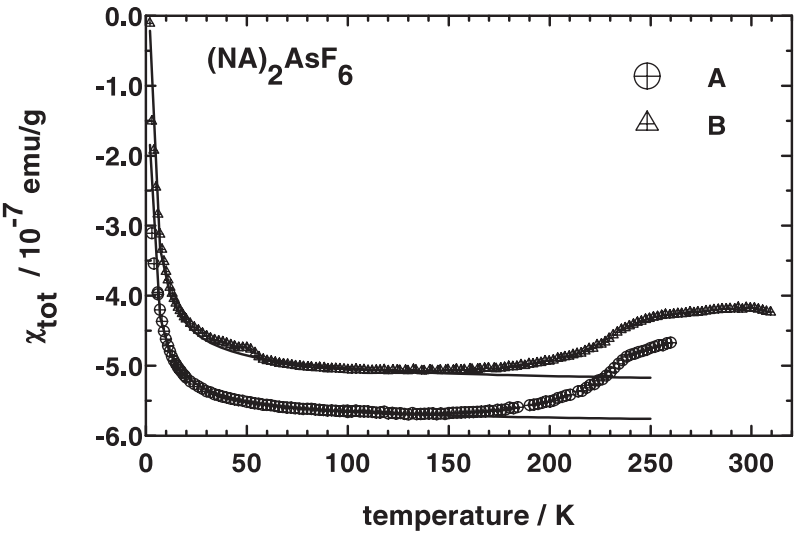

Figure 3. Total magnetic susceptibility for two different samples (A, B) consisting of unoriented $(NA)_2AsF_6$ crystals. The solid-curve fit is explained in the text. (The small anomaly around 50 K for sample B is caused by oxygen impurity in the sample space.)

The magnetic measurements were performed with a commercial Quantum Design MPMS SQUID magnetometer for several fixed field strength values and varied temperature, with the sample surrounded by helium atmosphere during the measurement.

3. Discussion of the results

3.1. Localized magnetic defects

Structural defects such as deviation from ideal stoichiometry or broken stacks give rise to localized paramagnetic defects in arene radical cation salts prepared by electrocrystallization. In addition, decomposition of aged crystals produces some radicals of arbitrary orientation. The influence of such paramagnetic defects is manifested by the low-temperature Curie tail of the total magnetic susceptibility (figure 3). The total magnetic susceptibility is decomposed according to equation (1):

$$\chi_{tot}(T) = \chi_{def}(T) + \chi_{dia} + \chi_c(T) \tag{1}$$

into contributions of paramagnetic defects, $\chi_{def}(T)$, temperature-independent molecular diamagnetism, χ_{dia}, and conduction electrons $\chi_c(T)$. The latter varies with temperature, in contrast to that for classical Pauli paramagnetism, due to the influence of the CDW fluctuation at $T > T_P$ and the opening of a static energy gap below the Peierls transition temperature T_P.

From a qualitative inspection of figure 3, the Curie tail of the $(NA)_2AsF_6$ samples A and B can be classified as of average strength. Using—irrespective of the actual composition of the sample—a molar mass $M_m = 445.3$ g corresponding to $(NA)_2AsF_6$, from the fitted value of

$$\chi_{def} = x N_A \frac{\mu_B^2}{k_B T} \tag{2}$$

we determine a concentration x of only about 1×10^{-3} $S = 1/2$ Curie defects per formula unit (table 1), at the lower end of the range of 3×10^{-4}–3×10^{-2} observed for other arene

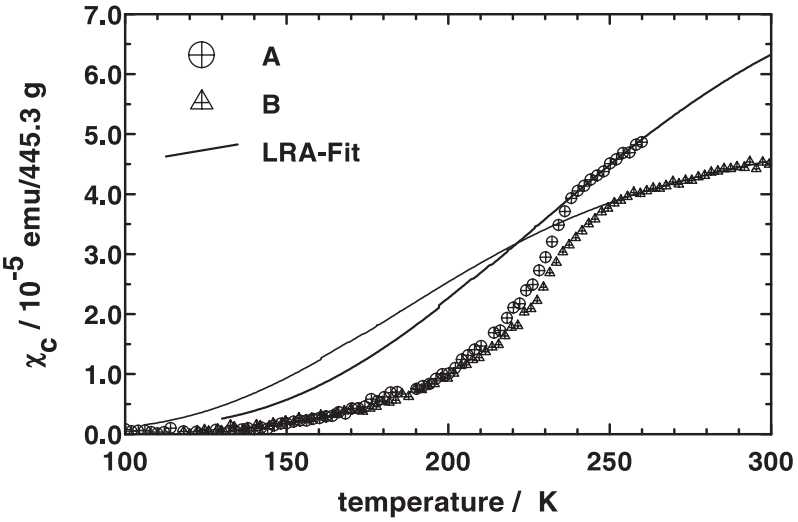

Figure 4. The conduction electron contribution to magnetic susceptibility for nominally one mol of $(NA)_2AsF_6$ ($M_m = 445.3$ g). The fit of the LRA model uses $\chi_P = 102.5 \times 10^{-6}$ (62.3×10^{-6}) emu mol^{-1} and $T_{MF} = 632$ (515) K for sample A (B).

salts [14–21]. Due to the tendency to decomposition, the ageing defects will be accumulated for the most part at the surface of the $(NA)_2AsF_6$ crystals. Thus a local defect concentration higher than $x = 1 \times 10^{-3}$ is expected, rendering exchange interaction of these defect spins possible. The solid curves in figure 3 show that the temperature dependence of the defect contribution can indeed be better described by a $\chi_{def}(T) = C/T^{\alpha}$ law, with $\alpha = 0.75$. This behaviour, explained by the REHAC (random exchange Heisenberg antiferromagnetic coupling) model [22] was also observed in case of higher defect concentrations for $(FA)_2PF_6$ salts [15].

3.2. Molecular diamagnetism

The fitted values of the molecular diamagnetism (table 1) can be used to estimate the degree of sample decomposition. Using the molar mass of $M_m = 445.3$ g of $(NA)_2AsF_6$ and the tabulated values of AsF_6 and NA diamagnetism [23, 24], we estimate $\chi_{dia}(\mathrm{NA}) = -7.3 \times 10^{-7}$ emu g^{-1} (average over all molecular orientations) and $\chi_{dia}((NA)_2AsF_6) = -5.84 \times 10^{-7}$ emu g^{-1}, to be compared with the observed values $-(5.87 \pm 0.25) \times 10^{-7}$ and $-(5.31 \pm 0.25) \times 10^{-7}$ emu g^{-1} for sample A and B, respectively (table 1). This indicates that the $(NA)_2AsF_6$ radical cation salt predominates clearly in this magnetic investigation (about 95% for sample A).

3.3. Conduction electron contribution

Figure 4 shows the separated conduction electron contribution $\chi_c(T)$ (equation (1)) for both samples. The solid curve shows the temperature dependence caused by CDW fluctuations according to the Lee–Rice–Anderson (LRA) model predictions [25]. In the LRA model, the temperature dependence of the magnetic susceptibility is parametrized by the 'infinite'-temperature limit of the Pauli paramagnetic susceptibility, χ_P, and a molecular field temperature T_{MF} characterizing the strength of electron–phonon coupling [25]. Due to the reduced dimensionality and the corresponding large influence of CDW fluctuations, no three-

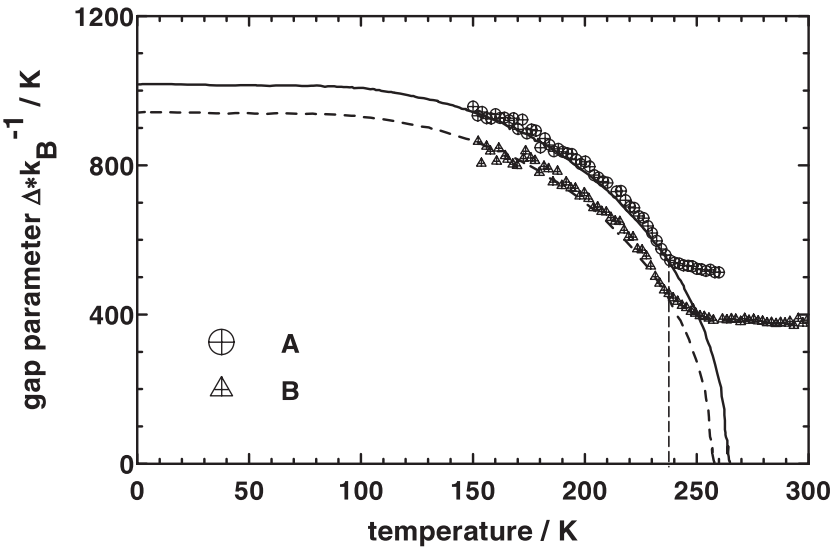

Figure 5. The temperature dependence of the effective or real gap parameter derived from the data of figure 4 with equation (3). The solid-curve and broken-curve fits show rescaled BCS-like variation (see the text). The vertical line indicates 'T_P'.

dimensional order is related to T_{MF}. Instead, the actual Peierls transition (at T_P) is expected to occur only at about $T_P \approx \frac{1}{4}T_{MF}$ [7, 25]. Since the data are analysed on the assumption that 445.3 g of the sample is equivalent to 1 mol of $(NA)_2AsF_6$, the derived high-temperature limiting value of the Pauli paramagnetism, i.e. $\chi_P = 102.5\ (62.3) \times 10^{-6}$ emu mol^{-1} $(NA)_2AsF_6$ for sample A (B) represents only a lower limit (table 1). On the other hand, the values of the molecular field temperature $T_{MF} = 632\ (515)$ K depend only on the relative variation and are thus insensitive to a possible error in the correct sample composition. Table 2 illustrates that this range of T_{MF}-values clearly is the highest one studied so far. Thus the tendency to undergo a Peierls transition and the influence of electron–phonon coupling favouring a doubling of the unit cell are the most pronounced for this naphthalene radical cation salt.

3.4. Opening of the energy gap

The data for $\chi_c(T)$ separated out above (figure 4) can be used to derive an effective energy gap for the high-temperature fluctuation regime and a real static gap for the low-temperature phase using [26]

$$\frac{\chi_c(T)}{\chi_P} = 2\int_A^\infty \frac{x}{\sqrt{x^2 - A^2}} \frac{e^x}{(e^x + 1)^2}\,dx \tag{3}$$

with $A = \Delta_{eff}/T$. With the help of equation (3), the experimentally accessible variation of $\chi_C(T)$ is modelled by the static (real) but temperature-dependent energy gap $2\Delta(T)$ of a one-dimensional semiconductor. The resulting variation of $\Delta(T)$ can be used to analyse thermodynamic data [26]. In addition, $\Delta(T)$ illustrates graphically the influence of high-temperature CDW-like fluctuations as compared to the real gap of the Peierls-distorted low-temperature phase below T_P. These results are shown in figure 5, in comparison to a rescaled BCS-like temperature dependence indicated as solid and broken curves (in contrast to the

standard BCS variation with $\Delta(0) = 1.76 \times k_B T_{MF}$, an arbitrary scaling factor was introduced for the numerical variation of $\Delta(T)/\Delta(0)$ versus T/T_P taken from [27]). It is evident that the actual Peierls transition temperature $T_P = 238$ K as well as the low-temperature extrapolations of the gap parameter $\Delta(0)/k_B = 1015$ and 940 K for samples A and B agree within the typical accuracy of this kind of analysis, irrespective of the problems with the sample stability discussed above. In figure 5, $T_P = 238$ K is appropriate for both samples A and B, consisting of many individual crystals. Since the opening of a static energy gap in a CDW–Peierls system influences the magnetic susceptibility as well as the electrical conductivity, T_P can be derived by microwave conductivity measurements, too. Since microwave conductivity measurements of an individual single crystal yield a Peierls transition temperature of about 230 K (determined from the transition anomaly in the temperature dependence of the conductivity [28]) we quote a Peierls transition temperature of $T_P = 234 \pm 4$ K for the $(NA)_2AsF_6$ salt.

4. Conclusions

In spite of the current magnetic analysis of a large number of slowly decomposing crystals [11, 12] originating from different electrocrystallization runs, the Peierls transition anomaly observed in the conduction electron magnetic susceptibility (figure 4) or in the effective energy gap (figure 5) of the naphthalene radical cation salt $(NA)_2AsF_6$ is well defined. The Peierls transition temperature $T_P = 234 \pm 4$ K is thus derived. As is familiar also from many inorganic one-dimensional conductors [29], or the fluoranthene radical cation salts [14], the molecular field temperature T_{MF} describing the influence of the high-temperature CDW-like fluctuations and the low-temperature limiting value of the static gap parameter $\Delta(0)$ follow closely the BCS-like relation $2\Delta(0) = 3.52 k_B T_{MF}$. Instead of 3.52, values of 3.21 and 3.65 are calculated for samples A and B, respectively (table 1).

On the other hand, the actual Peierls transition temperature T_P is substantially suppressed by a factor $T_P/T_{MF} = 0.37$ (0.45) for sample A (B). This is a well known observation for quasi-one-dimensional organic as well as inorganic conductors exhibiting CDW–Peierls transition (see table 2 for further examples). We refer the reader to the sources given in table 2 and to [7, 10, 25, 29] for further examples and discussion of the relevant theoretical attempts for a description. In this connection we should mention more recent efforts in the treatment of the spin–Peierls transition, too [30–32].

The high-temperature limiting value of the Pauli paramagnetism suffers more from the uncertainty in the actual sample composition (or decomposition). Nevertheless, the derived susceptibility of $\chi_P = (82.5 \pm 21) \times 10^{-6}$ emu/445.3 g seems smaller than the corresponding value of $\chi_P((FA)_2PF_6) = (135.5 \pm 5.5) \times 10^{-6}$ emu mol^{-1} derived for the fluoranthene radical cation salt with the same conduction band filling [14]. The bandwidth must be somewhat larger or the electron–electron interaction even weaker than in the latter salt. No *ab initio* electronic band-structure calculations for $(NA)_2AsF_6$ are currently available, however, and sample decomposition will prevent any reflection optical spectroscopical analysis in the future.

Table 2 summarizes our current information about the Peierls transition of various quasi-one-dimensional conductors belonging to the family of arene radical cation salts with octahedral hexafluoride complex anions PF_6, AsF_6, or SbF_6. The highest Peierls transition temperatures are observed for the simple stoichiometric naphthalene and fluoranthene salts, which have a three-quarter-filled conduction band in the extended band scheme, according to the molecular as well as the electronic (or ionic) 2:1 stoichiometry. Due to the packing peculiarities of the two groups of salts (PF_6 and AsF_6 salts behave similarly), two NA or FA molecules form the repetition unit in the stacking direction in the high-temperature phase which accordingly has a half-filled conduction band. Another doubling of the period length

in the stacking direction is thus required for the opening of the gap at the Fermi energy. The important role of the complex anions for the coupling of the one-dimensional fluctuations was established in the past [10]. This is most clearly demonstrated by comparison of the perylene radical cation salts. $(PE)_4(SbF_6)_3$ shows the largest value of the molecular field temperature T_{MF} among the three PE salts, but its transition temperature T_P is suppressed below 30 K due to disorder of the SbF_6 anion stacks [19]. Thus such structural details are more relevant for the value of the actual Peierls transition temperature of arene radical cation salts than simple band-filling arguments.

Acknowledgments

We thank I Odenwald for crystal growth and S Matejcek for microwave conductivity measurements. This work was financially supported by the Deutsche Forschungsgemeinschaft within the Sonderforschungsbereich 195 (Universität Karlsruhe).

References

[1] Voigt J 1995 *Rep. Prog. Phys.* **58** 977
[2] Zwick F, Grioni M, Margaritondo G, Vercoli V, Degiori L, Alavi B and Grüner G 2000 *Solid State Commun.* **113** 179
[3] Georges A, Giamarchi T and Sandler N 2000 *Phys. Rev.* B **61** 16 393
[4] Ilakovac V, Ravy S, Pouget J P, Rieß W, Brütting W and Schwoerer M 1993 *J. Physique Coll.* **3** IV C2 137
[5] Buschhaus C, Moret R, Ravy S and Dormann E 2000 *Synth. Met.* **108** 21
[6] Peierls R 1955 *Quantum Theory of Solids* (Oxford: Oxford University Press)
[7] Bartosch L 2001 *Ann. Phys., Lpz.* **10** 799
[8] Wokrina T, Dormann E and Kaplan N 1996 *Phys. Rev.* B **54** 10 492
[9] Tashma T, Alexandrowicz G, Kaplan N, Dormann E, Grayevsky A and Gabay A 1999 *Synth. Met.* **106** 151
[10] Desquiotz R, Hofmann M and Dormann E 2000 *Eur. Phys. J.* B **16** 403
[11] Fritz H P, Gebauer H, Friedrich P, Ecker P, Artes R and Schubert U 1978 *Z. Naturf.* b **33** 498
[12] Müller E, von Schütz J U and Wolf H C 1983 *J. Physique Coll.* **44** C3 1401
Müller E, von Schütz J U and Wolf H C 1983 *Mol. Cryst. Liq. Cryst.* **93** 407
[13] Enkelmann V 1988 *Adv. Chem. Ser.* **217** 177
[14] Köbler U, Gmeiner J and Dormann E 1987 *J. Magn. Magn. Mater.* **69** 189
[15] Dormann E and Sachs G 1987 *Ber. Bunsenges. Phys. Chem.* **91** 879
[16] Sachs G and Dormann E 1988 *Synth. Met.* **25** 157
[17] Dormann E 1988 *Synth. Met.* **27** B529
[18] Burggraf M, Dragan H, Gruner-Bauer P, Hellberg H W, Kuhs W F, Mattern G, Müller D, Wendl W, Wolter A and Dormann E 1995 *Z. Phys.* B **96** 439
[19] Buschhaus C, Desquiotz R, Eichhorn K, Hofmann M, Hümmer K, Illich V, Kelemen M, Tarragona Auga S, Wokrina T, Zitsch A and Dormann E 1999 *Eur. Phys. J.* B **8** 57
[20] Pongs B, Matejcek S, Kelemen M T, Buschhaus C and Dormann E 2001 *Synth. Met.* **120** 839
[21] Pongs B 2001 Elektronenspinresonanz an Pyrenradikalkationensalzen *PhD Thesis* (Aachen: Shaker)
[22] Tippie L C and Clark W G 1981 *Phys. Rev.* B **23** 5846
Tippie L C and Clark W G 1981 *Phys. Rev.* B **23** 5854
[23] Sellwood P W 1956 *Magnetochemistry* (New York: Interscience) p 78
[24] Weast R C and Astle M J (ed) 1980/81 *CRC Handbook of Chemistry and Physics* 61st edn (Boca Raton, FL: Chemical Rubber Company Press) p E-136
[25] Lee P A, Rice T M and Anderson P W 1973 *Phys. Rev. Lett.* **31** 462
[26] Johnston D C 1984 *Phys. Rev. Lett.* **52** 2049
[27] Brütting W, Rieß W and Schwoerer M 1992 *Ann. Phys., NY* **1** 409
[28] Matejcek S 2002 private communication
[29] Johnston D C, Maki M and Grüner G 1985 *Solid State Commun.* **53** 5
[30] Uhrig G S 1998 *Phys. Rev.* B **57** 14 004
[31] Gros C and Werner R 1998 *Phys. Rev.* B **58** 14 677
[32] Holicki M, Fehske H and Werner R 2001 *Phys. Rev.* B **63** 174417